RAA 2021 Vol. **21** No. **2**, 38(8pp) doi: 10.1088/1674-4527/21/2/38

http://www.raa-journal.org *http://iopscience.iop.org/raa*

***R**esearch in*
***A**stronomy and*
***A**strophysics*

Research on the panel adjustment method of an active main reflector for a large radio telescope

Zheng-Xiong Sun[1], Jin-Qing Wang[1,2,3], Lin-Feng Yu[1], Wei Gou[1] and Guang-Li Wang[1,4]

[1] Shanghai Astronomical Observatory, Chinese Academy of Sciences, Shanghai 200030, China; *zxsun@shao.ac.cn*
[2] Key Laboratory of Radio Astronomy, Chinese Academy of Sciences, Nanjing 210008, China
[3] Shanghai Key Laboratory of Space Navigation and Positioning Techniques, Shanghai 430074, China
[4] University of Chinese Academy of Sciences, Beijing 100049, China

Received 2020 June 12; accepted 2020 July 13

Abstract The surface accuracy of a large parabolic antenna is an important indicator to evaluate the quality of the antenna. It not only directly affects the antenna's aperture efficiency, thereby determining the shortest wavelength that the antenna can work, but also affects the main lobe width and side lobe structure of the antenna pattern. Microwave holography is an important method for parabolic antenna profile detection. In this article we adopt a new algorithm to adjust the panels for the large radio telescope with an active main reflector through the TM65 m antenna's aperture phase profile. The panels of the TM65 m radio telescope is in a radial pattern with 14 rings. Each corner of the panel is fixed on the screw of the actuator to move up and down, and the adjacent corners of the four panels share an actuator. We use the method of plane fitting to calculate the adjustment value of every panel's corner. But one actuator, which simultaneously controls the common corner of the adjacent panels, will have different adjustment values according to the different plane fitting equation based on adjacent panels. In this paper, the adjustment value of the adjacent panels'crosspoints are constrained to be equal to the constraint condition to calculate each actuator's adjustment value of the TM65 m radio telescope. Through multiple adjustments and application of the new algorithms, the accuracy of the TM65 m antenna reflector profile has been improved from the original 0.28 mm to the current 0.19 mm.

Key words: microwave holography — radio astronomy — surface deviation — least squares method

1 INTRODUCTION

With the continuous development of radio astronomy observation and deep space exploration technology, the requirements for antenna surface shape accuracy are increasing, especially for the establishment of a large aperture reflector antenna (Cortes-Medellin & Goldsmith 1994; Kamegai & Tsuboi 2013). The surface accuracy is not only affected by panel manufacture and assembly accuracy, but also by complex environmental factors such as its own gravity, temperature, and wind. In the process of observing the radio source, the panel shape of antenna will change in real time due to the gravity deformation of the antenna (Wang et al. 2017). It is necessary to adopt the adjustable main reflector system to regulate the main reflector shape of the antenna in real time according to the observation elevation angle at high frequencies (Greve & Karcher 2009; Wang et al. 2018). In order to measure the shape of the main reflector surface of the radio telescope, the theodolite measurement, total station measurement, laser tracking measurement, photogrammetry and other measurement technologies have appeared successively. However, these methods have the disadvantages of long measurement time, complicated operation, and can only be applied in a specific antenna attitude during the measurement process. Therefore, they cannot meet the application requirements of modern large diameter antennas. Microwave holography has the advantages of high measurement accuracy, comprehensive measurement effect and low measurement cost, and has been widely used in antenna surface inspection.

The phase recovery holography belongs to the category of microwave holography. Holographic measurement is an important method to measure the parabolic antenna profile. The basic principle of holographic method to measure the accuracy of the antenna reflector surface is to

obtain the amplitude and phase distribution of the antenna aperture field by measuring the amplitude and phase of the antenna far field, so as to calculate the deviation of the antenna reflector surface from the paraboloid (Wu 2015).

In order to quickly and accurately adjust the main reflector of a radio telescope, the new large diameter reflector antennas have successively adopted a main reflector control system to adjust every actuator, which also makes the adjustment of the antenna panel more rapid and convenient (Orfei et al. 2004; Wang et al. 2013; Nikolic et al. 2007). The TM65 m radio telescope is a full solid panel with an aperture diameter of 65 m. It was equipped with a sub-reflector which was driven by a six-bar mechanism to compensate for the defocusing caused by gravity deformation at high and low elevation angles (Sun et al. 2016). It was also equipped with an active reflector system, which was used to compensate for the decrease in efficiency due to gravity deformation of the main reflector at high and low elevation angles. The active reflector system of the TM65 m telescope is composed of 1104 actuators and a set of control systems. The 1104 actuators were installed on the back frame of the antenna. Each actuator has four screws on which the four corners of four adjacent panels were fixed. When the 1104 actuators move up and down, the 1008 panels also move accordingly.

In order to facilitate manufacture and installation for large reflector antennas, the main reflector is usually composed of multiple single panels. For the standard paraboloid reflector, the Fermat's principle shows that the optical path distance from the focus to the aperture plane is equal. Therefore, when electromagnetic waves radiated in any direction at the focus of the paraboloid are reflected by the standard paraboloid reflector surface, the wavefront phase value on the aperture field plane will be equal everywhere. However, the actual situation of the antenna panel is not the case. Due to factors such as the installation accuracy of the antenna panel and the gravity deformation of the support structure, the antenna panel is no longer a completely standard paraboloid, which will cause the phases on the aperture field plane to be not equal (Mazzarella et al. 2012). Thus, we can establish the relationship between the displacement of the actual paraboloid deviating from the standard paraboloid position and the phase difference on the aperture field plane. By checking this phase difference, it is theoretically possible to determine the reflector surface deformation. As the accuracy of the reflector surface decreases, the reflector efficiency of the panel will obviously decrease, which directly affects the aperture efficiency of the radio telescope, especially the performance of the radio telescope working at high frequencies (Cheng 1955). For a parabolic antenna with a surface accuracy of ε (mm), the relationship between the effect of the surface error on the efficiency and the wavelength can be simply expressed as Equation (1) (Ruze 1952; Schanda 1967).

$$\eta_s = \exp\left[-\left(\frac{4\pi\varepsilon}{\lambda}\right)^2\right], \tag{1}$$

where λ is the wavelength. Therefore, with the same surface accuracy, the antenna efficiency at high-frequency is much lower than that at low-frequency, and the panels of antenna need to be adjusted in real time during observation at high-frequency.

2 MICROWAVE HOLOGRAPHIC MEASUREMENT

The surface accuracy of a large paraboloid antenna not only directly affects the antenna's aperture efficiency, but also affects the main lobe width and side lobe structure of the antenna pattern. Thus, accurate measurement of surface accuracy is of great importance for a reflector antenna. Holographic measurement is an important method to measure the parabolic antenna profile. The basic principle of the holographic method to measure the accuracy of the antenna surface is to obtain the amplitude and phase distribution of the antenna aperture field by measuring the amplitude and phase of the antenna far field, so as to calculate the deviation of the antenna reflector surface from the paraboloid (Rahmat-Samii 1985; Scott & Ryle 1977).

The aperture phase is uniform for a perfect paraboloidal reflector. Departure from uniformity can be related to errors in the reflector profile using the geometrical optics construction shown in Figure 1. From the enlarged view, the total path length change of the ray is as Equation (2).

$$\delta_r + \delta_p = \frac{\varepsilon}{\cos\eta} + \frac{\varepsilon\cdot\cos 2\eta}{\cos\eta}. \tag{2}$$

For a parabolic antenna, the distance ρ from the focal point to any point on the reflector surface can be expressed as:

$$\rho = \frac{2F}{1+\cos 2\eta} = \frac{\sqrt{x^2+y^2}}{\sin 2\eta}, \tag{3}$$

where x and y is the plane projection coordinate of the point on the reflector surface; 2η is the opening angle of this point.

The cosine function of angle η can be derived from Equation (3):

$$\cos\eta = \frac{2F}{\sqrt{x^2+y^2+4F^2}}. \tag{4}$$

So the relationship between reflector surface error ε and the aperture phase φ is Equation (5). λ is the working wavelength.

$$\varphi = 2\pi\cdot\frac{2\varepsilon\cdot\cos\eta}{\lambda}. \tag{5}$$

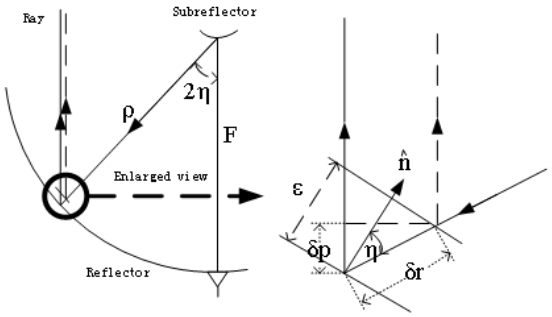

Fig. 1 The effect of a small normal surface error ε on the ray path from the feed to the aperture plane.

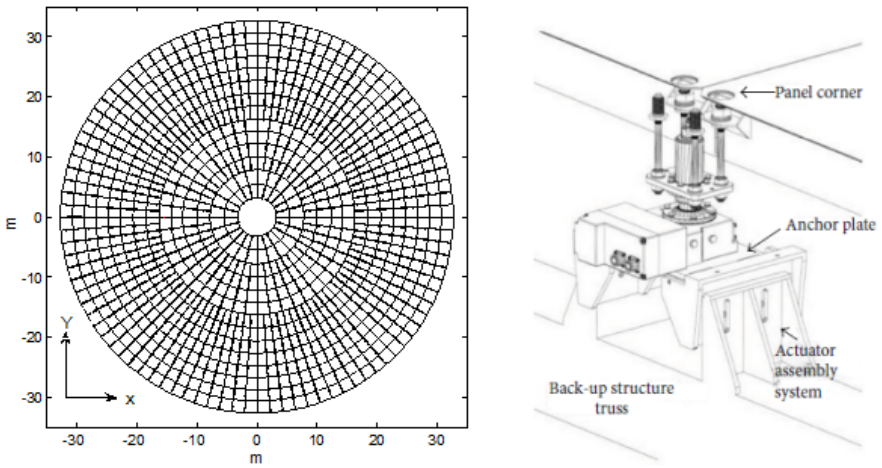

Fig. 2 Left is main reflector of the TM65 m; right is the actuator installed on back frame of the TM65 m.

The theoretical basis of holographic measurement is that there is a two-dimensional Fourier transform relationship between the aperture field and the far field of the parabolic antenna. In actual situations, the antenna reflector will not be a perfectly ideal parabolic surface, so the phase on the aperture plane must also be unequal. When the signal wavelength is determined, by measuring this phase difference, the deviation of the antenna reflector can be determined. The electromagnetic field theory and Fourier transform theory can be used to deduce the relationship between the antenna's radiated far field and the antenna surface tolerance (Bennett et al. 1976):

$$\varepsilon\left(x,y\right)=\frac{\lambda}{4\pi}\sqrt{1+\frac{x^2+y^2}{4F^2}}\,\mathrm{phase}\left\{e^{j2kF}F^{-1}\left[T(u,v)\right]\right\}, \tag{6}$$

where $\varepsilon(x,y)$ is deformation of reflector antenna panels; x and y are normalized aperture coordinates points on the reflector antenna; F is the normalized equivalent parabolic focal length of reflector antenna; phase is the obtained phase of the aperture field; k is the propagation constant; $F^{-1}[\cdots]$ is the inverse two-dimensional Fourier transform; $T(u,v)$ is the remote radiation field of a reflector antenna (Yin et al. 2000).

3 ACTIVE REFLECTOR COMPENSATION CALCULATION

The main reflector of the TM65 m radio telescope is composed of 14 rings panels. The inner diameter of the 1st ring panels is 3.199 m, and the outer diameter of the 14th ring panels is 32.5 m. The 1st ring and the 2nd ring each consist of 24 pieces of panels. The 3rd ring to the 6th ring each consist of 48 pieces of panels, and the 7th to the 14th ring each consist of 96 pieces panels, as shown in Figure 2 below. Each cosspoint in the picture is supported by an actuator.

3.1 Calculating the Adjustment Value of the Four Corners of the Panels by Plane Fitting

The ultimate purpose of holographic measurement is to provide the antenna user where and how much to adjust the antenna surface (to raise or lower the panels). We obtained the profile distribution through holographic measurement.

In the case of the two-dimensional inverse Fourier transform, the required observation data are points strictly distributed on the far field grid. In fact, the observation

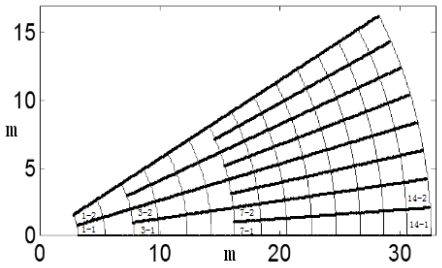

Fig. 3 Number index map of the main reflector surface of TM65m radio telescope.

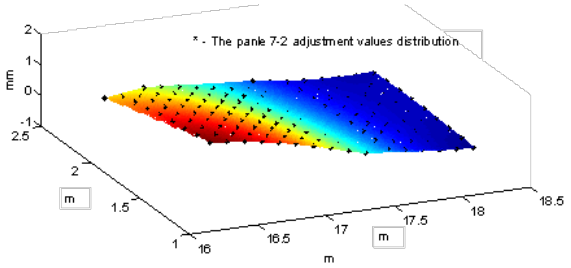

Fig. 4 The adjustment values distribution of the panel 7-2.

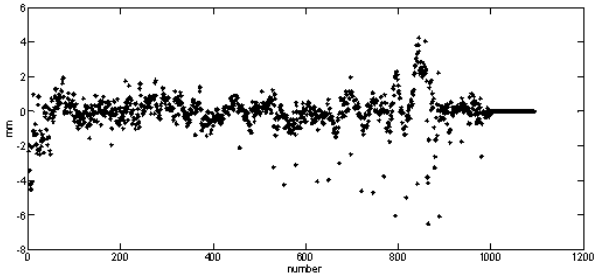

Fig. 5 The adjustment values of the 1104 actuators.

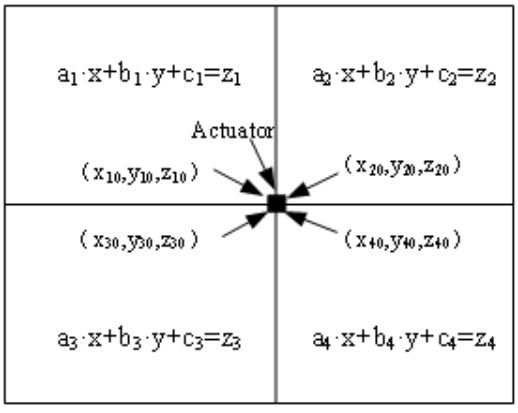

Fig. 6 The schematic diagram of four adjacent panels.

data cannot be ideally distributed. The "grid" process is to map the actual observation data to a strict far field grid by mathematical means. In order to use the fast two-dimensional inverse Fourier transform algorithm, such grid points need to be set to an integer power of two.

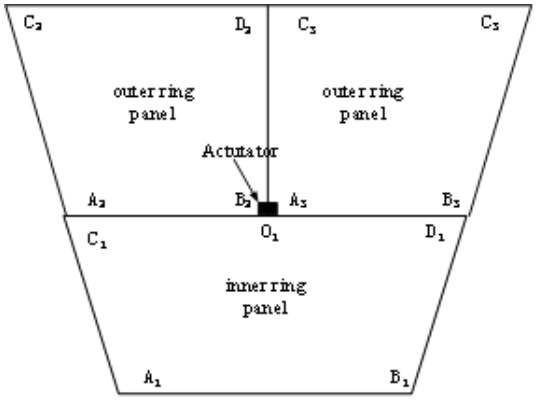

Fig. 7 Top view of panel; showing the 3rd ring or the 7th ring actuators with an even number index connected two rings panels.

A matrix of 512× 512 is obtained from the holographic measurement of the main reflector surface for the TM65 m radio telescope.

In order to find the adjustment value of a specific panel, the value of the 512 × 512 data matrix must first be mapped to each panel. The panel distribution is indexed with two variables. The number of ring is the first-level index, which starts horizontally to the right. The number of piece for a specific panel is the second-level index, which counted counterclockwise, as shown in Figure 3, an example of panels, in a radial pattern with 14 rings; shows 1/12 of reflector.

For example, we need to find the adjustment data corresponding to the panel 7-2. First, we let the coordinates points of each data in the 512 × 512 matrix multiply a scale factor 65/512 to normalize the actual aperture coordinate position of the antenna reflector surface. Thus the adjustment data corresponding to the panels can be found according to the starting/ending angles of the panel edge and the inner/outer diameters of the panel. Since the 7th ring consists of 96 panels and the inner diameter is 16.249 m and the outer diameter is 18.431 m. In addition, the opening angle of each panel in the 7th ring is 3.75 degrees. So the starting angle and ending angle of the panel 7-2 respectively are 3.75 degrees and 7.5 degrees. Finally, the 153 adjustment data obtained from the 512× 512 data matrix is distributed on the panel 7-2, as shown in Figure 4.

At first, after obtaining the above results, the antenna engineer averaged those values as the adjustment value at the four corners of one panel and then averaging the adjustment values at crosspoint of the four adjacent panels. Since each reflector panel of the TM65 m radio telescope with four adjustment screws is a steel plate, we can use least squares method to plane fitting these data to get the adjustment values at four corners of the panel, and then averaging the adjustment values at crosspoint of adjacent

panels. TM65 m is currently using this method to obtain the adjustment value of each actuator. Equation (7) is the plane equation.

$$a \cdot x + b \cdot y + c = z \tag{7}$$

where a, b and c are the unknown coefficient to be sought; and x, y and z are the coordinate value of the point in Figure 4. In the program, the three unknown parameters are solved by the Gaussian elimination using the least squares method through matrix Equation (8). Suppose the left matrix is A and the right matrix is B, so $[a,b,c]^T$=A^{-1}·B. N indicates the number of adjustment data mapped on this reflector panel.

$$\begin{bmatrix} \sum_{i=1}^{i=N} x_i^2 & \sum_{i=1}^{i=N} x_i \cdot y_i & \sum_{i=1}^{i=N} x_i \\ \sum_{i=1}^{i=N} x_i \cdot y_i & \sum_{i=1}^{i=N} y_i^2 & \sum_{i=1}^{i=N} y_i \\ \sum_{i=1}^{i=N} x_i & \sum_{i=1}^{i=N} y_i & N \end{bmatrix} \cdot \begin{bmatrix} a \\ b \\ c \end{bmatrix} = \begin{bmatrix} \sum_{i=1}^{i=N} x_i \cdot z_i \\ \sum_{i=1}^{i=N} y_i \cdot z_i \\ \sum_{i=1}^{i=N} z_i \end{bmatrix} \tag{8}$$

We can calculate the adjustment value at each corner according to Equation (7). Besides, the coordinates of points of the four corners of the panel are easier to get. Obviously the crosspoint adjustment values of the four adjacent panels are four different values separately solved in four different plane equations. How to adjust the actuator based on these four values calculated at the same point is a problem. In general, the average value of these four values will be used as the basis for adjusting the actuator at this point. The calculation results are shown in Figure 5. The ordinate in the figure is the adjustment value of actuator, and the abscissa is the number of the actuator. It can be seen from the figure that the adjustment values of individual actuators are relatively large because part of the panels are obscured by the support legs which support the sub-reflector. Due to the accuracy sharp deterioration of the holographic measurement at the edge area, the measurement of the last ring panel is not accurate. TM65 m used 1104 actuators to adjust the main surface shape. By means of the method of plane fitting to repeatedly measure and adjust, and finally the surface profile accuracy gradually increased to 0.28 mm (RMS). The result deducts the obscured part of the sub-reflector support legs and the outermost panels.

3.2 Calculating the Adjustment Value with Constraints

Adjusting an actuator based on the average value calculated by the four different plane equations above is not the best adjustment method. We add a constraint on the basis of the above plane fitting, namely, the z value at the crosspoint of the four adjacent panels are equal, as shown in Figure 6. We use z_{10} = z_{20} = z_{30} = z_{40} as a constraint to plane fitting equation of four adjacent panels.

In order to calculate the optimal adjustment value of the actuator, Equation (9) needs to be satisfied to solve the plane fitting parameters for minimizing the δ value. z_0 is the adjustment value of the actuator and (x_0,y_0) is the known coordinate point:

$$\begin{cases} f_1 : a_1 \cdot x_{10} + b_1 \cdot y_{10} + c_1 - z_{10} = 0 \\ f_2 : a_2 \cdot x_{20} + b_2 \cdot y_{20} + c_2 - z_{20} = 0 \\ f_3 : a_3 \cdot x_{30} + b_3 \cdot y_{30} + c_3 - z_{30} = 0 \\ f_4 : a_4 \cdot x_{40} + b_4 \cdot y_{40} + c_4 - z_{40} = 0 \\ x_{10} = x_{20} = x_{30} = x_{40} = x_0 \\ y_{10} = y_{20} = y_{30} = y_{40} = y_0 \\ z_{10} = z_{20} = z_{30} = z_{40} = z_0 \end{cases} \tag{9}$$

$$\begin{aligned} \delta = & \sum_{i=1}^{i=N} (a_1 \cdot x_{1i} + b_1 \cdot y_{1i} + c_1 - z_{1i})^2 \\ & + \sum_{i=1}^{i=N} (a_2 \cdot x_{2i} + b_2 \cdot y_{2i} + c_2 - z_{2i})^2 \\ & + \sum_{i=1}^{i=N} (a_3 \cdot x_{3i} + b_3 \cdot y_{3i} + c_3 - z_{3i})^2 \\ & + \sum_{i=1}^{i=N} (a_4 \cdot x_{4i} + b_4 \cdot y_{4i} + c_4 - z_{4i})^2 \end{aligned} \tag{10}$$

where (x_{1i},y_{1i},z_{1i}) represents the coordinate values of the holographic measurement points in the 1st panel. N indicates the number of points on this reflector panel. a_1, b_1 and c_1 are plane fitting parameters of the panel. So the Lagrangian function to solve this problem is Equation (11):

$$F(a, b, c, \lambda, z_0) = \delta + \lambda_1 \cdot f_1 + \lambda_2 \cdot f_2 + \lambda_3 \cdot f_3 + \lambda_4 \cdot f_4 \tag{11}$$

where $\lambda_1, \lambda_2, \lambda_3, \lambda_4$ is the parameter, let the first order partial derivative of F with respect to the variables of the function be equal to zero.

$$\begin{cases} \frac{\partial F}{\partial a_1} = \sum_{i=1}^{i=N} 2 \cdot x_{1i} \cdot (a_1 \cdot x_{1i} + b_1 \cdot y_{1i} + c_1 - z_{1i}) + x_{10} \cdot \lambda_1 = 0 \\ \frac{\partial F}{\partial b_1} = \sum_{i=1}^{i=N} 2 \cdot y_{1i} \cdot (a_1 \cdot x_{1i} + b_1 \cdot y_{1i} + c_1 - z_{1i}) + y_{10} \cdot \lambda_1 = 0 \\ \frac{\partial F}{\partial c_1} = \sum_{i=1}^{i=N} 2 (a_1 \cdot x_{1i} + b_1 \cdot y_{1i} + c_1 - z_{1i}) + \lambda_1 = 0 \\ \frac{\partial F}{\partial a_2} = \sum_{i=1}^{i=N} 2 \cdot x_{2i} \cdot (a_2 \cdot x_{2i} + b_2 \cdot y_{2i} + c_2 - z_{2i}) + x_{20} \cdot \lambda_2 = 0 \\ \frac{\partial F}{\partial b_2} = \sum_{i=1}^{i=N} 2 \cdot y_{2i} \cdot (a_2 \cdot x_{2i} + b_2 \cdot y_{2i} + c_2 - z_{2i}) + y_{20} \cdot \lambda_2 = 0 \\ \frac{\partial F}{\partial c_2} = \sum_{i=1}^{i=N} 2 (a_2 \cdot x_{2i} + b_2 \cdot y_{2i} + c_2 - z_{2i}) + \lambda_2 = 0 \\ \frac{\partial F}{\partial a_3} = \sum_{i=1}^{i=N} 2 \cdot x_{3i} \cdot (a_3 \cdot x_{3i} + b_3 \cdot y_{3i} + c_3 - z_{3i}) + x_{30} \cdot \lambda_3 = 0 \\ \frac{\partial F}{\partial b_3} = \sum_{i=1}^{i=N} 2 \cdot y_{3i} \cdot (a_3 \cdot x_{3i} + b_3 \cdot y_{3i} + c_3 - z_{3i}) + y_{30} \cdot \lambda_3 = 0 \\ \frac{\partial F}{\partial c_3} = \sum_{i=1}^{i=N} 2 (a_3 \cdot x_{3i} + b_3 \cdot y_{3i} + c_3 - z_{3i}) + \lambda_3 = 0 \\ \frac{\partial F}{\partial a_4} = \sum_{i=1}^{i=N} 2 \cdot x_{4i} \cdot (a_4 \cdot x_{4i} + b_4 \cdot y_{4i} + c_4 - z_{4i}) + x_{40} \cdot \lambda_4 = 0 \\ \frac{\partial F}{\partial b_4} = \sum_{i=1}^{i=N} 2 \cdot y_{4i} \cdot (a_4 \cdot x_{4i} + b_4 \cdot y_{4i} + c_4 - z_{4i}) + y_{40} \cdot \lambda_4 = 0 \\ \frac{\partial F}{\partial c_4} = \sum_{i=1}^{i=N} 2 (a_4 \cdot x_{4i} + b_4 \cdot y_{4i} + c_4 - z_{4i}) + \lambda_4 = 0 \\ \frac{\partial F}{\partial \lambda_1} = (a_1 \cdot x_{10} + b_1 \cdot y_{10} + c_1 - z_0 = 0 \\ \frac{\partial F}{\partial \lambda_2} = (a_2 \cdot x_{20} + b_2 \cdot y_{20} + c_2 - z_0 = 0 \\ \frac{\partial F}{\partial \lambda_3} = (a_3 \cdot x_{30} + b_3 \cdot y_{30} + c_3 - z_0 = 0 \\ \frac{\partial F}{\partial \lambda_4} = (a_4 \cdot x_{40} + b_4 \cdot y_{40} + c_4 - z_0 = 0 \\ \frac{\partial F}{\partial z_0} = \lambda_1 + \lambda_2 + \lambda_3 + \lambda_4 = 0 \end{cases} \tag{12}$$

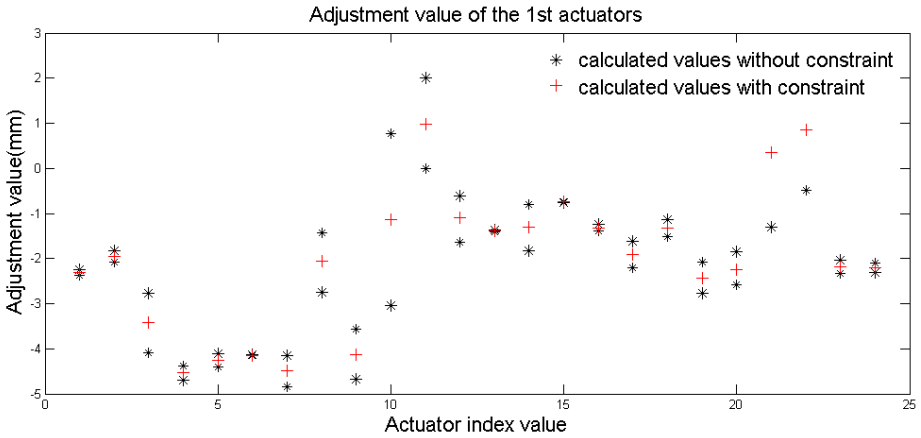

Fig. 8 Adjustment values of the 1st ring actuators.

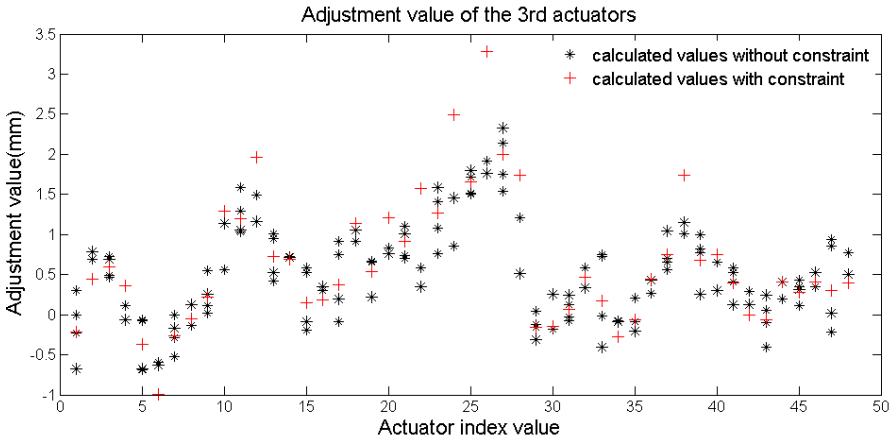

Fig. 9 Adjustment values of the 3rd ring actuators.

Using the formulas in lines 1, 2, 3 and 13 of Equation (12), the function of the 1st panel can be obtained, see Equation (13). In the same way, we can get the functional expressions of the 2nd, 3rd and 4th panels.

$$\begin{bmatrix} \sum_{i=1}^{i=N} x_{1i}^2 & \sum_{i=1}^{i=N} x_{1i}\cdot y_{1i} & \sum_{i=1}^{i=N} x_{1i} \\ \sum_{i=1}^{i=N} x_{1i}\cdot y_{1i} & \sum_{i=1}^{i=N} y_{1i}^2 & \sum_{i=1}^{i=N} y_{1i} \\ \sum_{i=1}^{i=N} x_{1i} & \sum_{i=1}^{i=N} y_{1i} & N \end{bmatrix} \cdot \begin{bmatrix} a_1 \\ b_1 \\ c_1 \end{bmatrix} = \begin{bmatrix} \sum_{i=1}^{i=N} x_{1i}\cdot z_{1i} \\ \sum_{i=1}^{i=N} y_{1i}\cdot z_{1i} \\ \sum_{i=1}^{i=N} z_{1i} \end{bmatrix} - \lambda_1 \cdot \begin{bmatrix} \frac{x_0}{2} \\ \frac{y_0}{2} \\ \frac{1}{2} \end{bmatrix} \tag{13}$$

where, suppose the left matrix is A and the right matrix is B. So $[a_1,b_1,c_1]^T = A^{-1}\cdot B - \lambda_1\cdot(A^{-1}\cdot[x_0/2,y_0/2,1/2]^T)$. Compared with Equation (8), therefore, the plane fitting coefficient calculated with constraints can be $a_1 = a_{10} - \alpha_1\cdot\lambda_1$, $b_1 = b_{10} - \beta_1\cdot\lambda_1$, $c_1 = c_{10} - \gamma_1\cdot\lambda_1$. Thus, a_{10} is the coefficient of plane fitting without constraints, which has been obtained before, and α_1, β_1 and γ_1 can be calculated. It can be obtained from the last five lines of Equation (12).

$$\begin{cases} (a_{10}\cdot x_0 + b_{10}\cdot y_0 + c_{10}) - \lambda_1\cdot(\alpha_1\cdot x_0 + \beta_1\cdot y_0 + \gamma_1) \\ (a_{20}\cdot x_0 + b_{20}\cdot y_0 + c_{20}) - \lambda_2\cdot(\alpha_2\cdot x_0 + \beta_2\cdot y_0 + \gamma_2) \\ (a_{30}\cdot x_0 + b_{30}\cdot y_0 + c_{30}) - \lambda_3\cdot(\alpha_3\cdot x_0 + \beta_3\cdot y_0 + \gamma_3) \\ (a_{40}\cdot x_0 + b_{40}\cdot y_0 + c_{40}) - \lambda_4\cdot(\alpha_4\cdot x_0 + \beta_4\cdot y_0 + \gamma_4) \\ \lambda_1 + \lambda_2 + \lambda_3 + \lambda_4 = 0 \end{cases} \tag{14}$$

where, the subscript 1,2,3 and 4 refers to the serial number of the four trapezoidal panels. According to Equation (14), z_0 can be calculated, which is the adjustment value of the actuator.

The TM 65 m radio telescope has 15 rings actuators, as shown in Figure 2. Each actuator at the corner of the 1st and 15th rings controls two adjacent panels. We call the two rings of adjacent panels connected to the actuator as the inner ring panel and the outer ring panel respectively. For the 3rd ring and 7th ring actuators with an even number index, it is not connected to the inner ring panel , but tangent with the outer edge of the inner ring panel at the middle position (O_1), as shown in Figure 7. In addition, it is connected to the corner of two panels on the outer ring (B_2 and A_3). However, for the 3rd ring and 7th ring

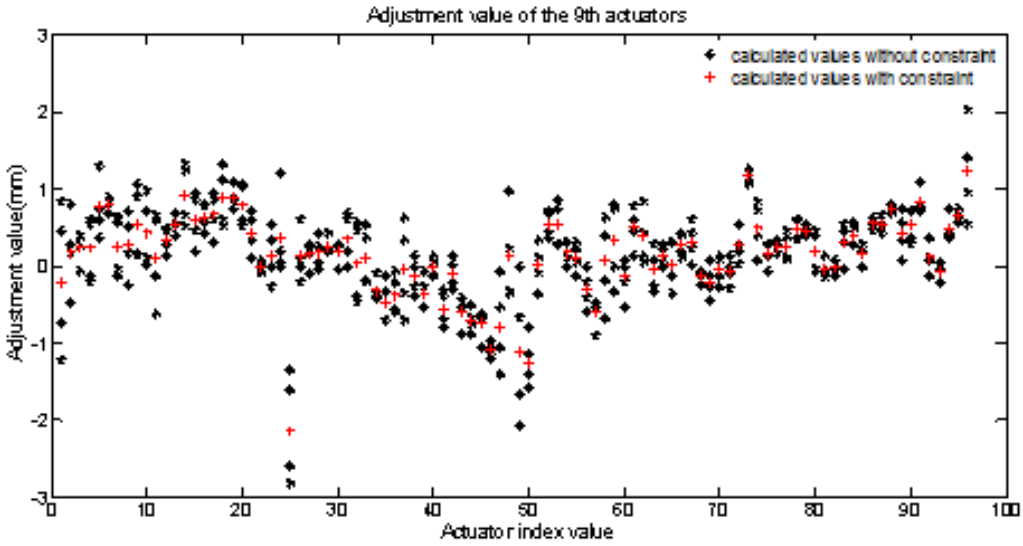

Fig. 10 Adjustment values of the 9th ring actuators.

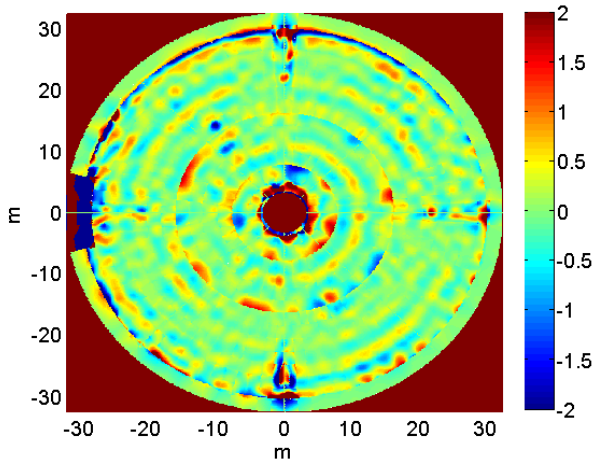

Fig. 11 The reflector accuracy after active panel adjustment, RMS=0.19mm.

actuators with odd number index, it is connected to the four adjacent panels (see Figure 6). When adjusting the actuator (up or down) in Figure 7, the inner panel will not be raised or lowered. Therefore, when calculating the adjustment value of the actuator, we must also consider the O_1 point that is not connected to the actuator. In the process of calculating the actuator adjustment values through the holographic measurement of the TM65 m radio telescope, we set the adjustment values of the three point coordinates (B_2, A_3 and O_1) to be equal as the constraint condition to plane fitting each panel for finding the actuator's best adjustment value. During programming, it is necessary to pay attention to the index number of each ring actuator when the number of inner and outer rings panels connected to the actuator is not equal. Calculating the adjustment value of the actuator connected to three intersection points or two intersection points, which make them equal to the constraint condition, is the same as the previous method for calculating the value of the actuator with four points equal to the constraint condition.

Figure 8 shows the comparison of the 1st ring actuators adjustment values, which is respectively calculated by plane fitting of a single panel alone to obtain the corner adjustment value and plane fitting with constraints where corner adjustment points of adjacent panels are equal. Figure 9 shows the comparison of the 3rd ring actuators adjustment values, where odd number index actuators are connected to the corners of four panels, and even number index actuators are connected to the corners of two panels but the tangent with the outer edge of the inner ring panels at the middle position. Figure 10 shows the comparison of the 9th ring actuators adjustment values, where corner adjustment values respectively in the four adjacent panels will have four different values. Actually, in the calculation

we obtain the corner adjustment values by plane fitting with constraints that corner adjustment points of adjacent panels is equal.

From the calculation results, the adjustment values of the actuators with constraint conditions are between several adjustment values which are obtained by calculating adjustment values of each panel separately. It can be seen from Figure 9 that the adjustment values of some even number index actuators are outside the range, that is because the adjustment values at point O_1(It is not controlled by the actuator) in Figure 7 is not displayed. Use the method with constraints to calculate the adjustment value of TM65 m actuator for the data obtained from the previous measurement, and finally obtain the surface shape accuracy of 0.19 mm (RMS), see Figure 11.

The decrease in the measurement accuracy of the outer ring panel is mainly caused by two reasons: first, the illumination function of the TM65m radio telescope falls on the edge, and the measurement accuracy will be reduced due to the decrease in the signal-to-noise ratio (SNR). Second, the outer edge of the back frame is more affected by the environment. Therefore, we regard the data of the outermost panel as invalid data.

4 SUMMARY

The term radio holography is generally used for any method to measure the phase distribution of the reflector aperture field and to identify deviations from the expected function with local distortions in the prescribed profile shape of the reflector. The paper focuses on the active main reflector. First, the relationship between the aperture phase of radio telescope and the panel deviation was calculated. The surface adjustment algorithm based on plane fitting with constraints, which take into account the fact that four panels use the same actuator and make the adjustment of adjacent panels continuous to avoid abnormal adjustment of a single panel. This new algorithm for calculating the adjustment value of the actuators has finally obtained satisfactory results, which provide a reference for other large radio telescopes with active surface systems.

References

Bennett, J. C., Anderson, A. P., McInnes, P. A., & Whitaker, A. J. T. 1976, IEEE Transactions on Antennas and Propagation, 24, 295

Cheng, D. 1955, IEEE Transactions on Antennas and Propagation, 3, 145

Cortes-Medellin, G., & Goldsmith, P. F. 1994, IEEE Transactions on Antennas and Propagation, 42, 176

Greve, A., & Karcher, H. J. 2009, IEEE Proceedings, 97, 1412

Kamegai, K., & Tsuboi, M. 2013, PASJ, 65, 21

Mazzarella, G., Montisci, G., & Serra, G. 2012, International Journal of Antennas and Propagation, 2012, 11

Nikolic, B., Prestage, R. M., Balser, D. S., Chand ler, C. J., & Hills, R. E. 2007, A&A, 465, 685

Orfei, A., Morsiani, M., Zacchiroli, G., et al. 2004, in Society of Photo-Optical Instrumentation Engineers (SPIE) Conference Series, 5495, Astronomical Structures and Mechanisms Technology, eds. J. Antebi, & D. Lemke, 116

Rahmat-Samii, Y. 1985, IEEE Transactions on Antennas and Propagation, 33, 1194

Ruze, J. 1952, Il Nuovo Cimento, 9, 364

Schanda, E. 1967, IEEE Transactions on Antennas and Propagation, 15, 471

Scott, P. F., & Ryle, M. 1977, MNRAS, 178, 539

Sun, Z.-X., Wang, J.-Q., & Chen, L. 2016, RAA (Research in Astronomy and Astrophysics), 16, 119

Wang, C. S., Li, J. J., Zhu, M, B., et al. 2013, Electro-Mechanical Engineering, 29, 5, (in Chinese)

Wang, C. S., Xiao, L., Xiang, B. B., et al. 2017, Scientia Sinica, https://doi.org/10.1360/SSPMA2017-00011

Wang, C., Li, H., Ying, K., et al. 2018, International Journal of Antennas & Propagation, 2018, 1

Wu, T. K. 2015, Microwave and Optical Technology Letters, 14, 221

Yin, X. H., Zhi cai, X. U., Han, F., Jing, L., & Lei, C. M. 2000, Chinese Journal of Radio Science, 02 (in Chinese)